Spectroscopic identification of active centers and reaction pathways on MoS2 catalyst for H 2 production via water-gas shift reaction

Weitao Zhao, Françoise Maugé, Jianjun Chen, Laetitia Oliviero

Spectroscopic identification of active centers and reaction pathways on MoS_2 catalyst for H_2 production via water-gas shift reaction

Weitao Zhao[1], Françoise Maugé[1], Jianjun Chen[2] and Laetitia Oliviero[1]*

1 Normandie Université, ENSICAEN, UNICAEN, CNRS, LCS, 14000 Caen, France

2 School of Environment, Tsinghua University, Beijing 100084, China

KEYWORDS: S/O exchange • sulfur vacancy • MoS_2 edges • reaction mechanism • structure-activity relationships • deactivation.

ABSTRACT

In previous reports, it was proposed that the oxygen-substituted $Mo(S_xO_y)_{zc}$ site formed *in situ* by water is active center for water-gas shift reaction catalyzed by MoS_2. However, water is also hypothesized to be the driving force for sulfide catalyst deactivation. This irreconcilable dispute stems from the limited understanding about the reaction mechanism and the lack of relevant *in situ* or/and *operando* characterization. In this work, the different reactivity of the two preferentially exposed MoS_2 edge sites, M-edge and S-edge sites, with CO and H_2O is revealed by means of *in situ* CO adsorption followed by IR spectroscopy. Isotopic reactants ($^{13}CO/^{12}CO$; $H_2{}^{18}O$) were used to account for the origin of the formed products and catalyst surface modification. In particular, upon H_2O feed, S/O exchange occurs

on M-edge leading to $Mo(S_xO_y)_{zc}$ sites that are not reactive towards subsequent CO feed in contradiction with a redox mechanism in which the catalyst surface is first exchanged by H_2O and then reduced by CO. Moreover, the M-edge sites hardly give vacancy under CO treatment. Conversely, the S-edge sites are much less prone to S/O exchange upon H_2O feed but are sensitive to CO to form vacancies and release COS. In addition, IR *operando* studies are in accordance with a formate pathway and a novel redox mechanism via COS formation. This insight into the catalytic active sites under reaction conditions allows to identify the M-edge sites as the ones leading to the deactivation of the catalyst and the S-edge sites as the redox active sites. Thus, the work gives the direction for the rational design of high-performance and stable sulfide catalysts for reactions involving H_2O dissociation and CO conversion.

1. Introduction

Molybdenum-based sulfide catalysts find extensive applications in various catalytic processes such as hydrodesulfurization, CO_2 hydrogenation as well as hydrogen production by water electrolysis and the water gas shift (WGS) reaction [1-5]. The catalytic activity for MoS_2 has been reported to mainly arises from the coordinatively unsaturated sites located along the edge of MoS_2 slabs rather than the saturated-coordination sites in basal plane [6, 7]. However, with the development of characterization technology, the understanding of active sites has also changed. Recently, in-plane sulfur atoms can be substituted by oxygen atoms doped into the MoS_2 [8-10], and this formed $MoS_{2-x}O_x$ sites can also act as active sites for hydrogen evolution reaction (HER) due to its good electrical conductivity [11]. Similarly, the importance of $MoS_{2-x}O_x$ site formed *in situ* as a result of hydrolysis has been recognized momentously for WGS reaction, and hitherto it has been proposed as an active center reacting with CO to release CO_2 [12, 13]. However, due to the lack of the sophisticated *in situ* characterization techniques on supported MoS_2 catalysts, this hypothesis involving $MoS_{2-x}O_x$ site as WGS active center is not yet fully experimentally verified and thus understanding the actual surface reaction at surface of MoS_2 should be significant deepened.

Another ambiguous issue is the comparative study of edge sites for their catalytic reactivity. Theoretical and experimental studies reveal the existence of two types of low-index edge terminations with different coordination environment over MoS_2 slab, i.e. the $(10\bar{1}0)$ M edge and the $(\bar{1}010)$ S edge [4, 14-17]. Such different coordination structures in M- and S-edge sites determine that they would have different reactivity. This point has been demonstrated in thiophene HDS reaction for which the intrinsic activity of S-edge sites is higher than that of M-edge sites [4]. However, for HER and WGS reaction, the comparative study of the two edge sites activity is experimentally rare, and most of the studies mainly focus on theoretical calculation. For instance, comparing the hydrogen bond energy, hydrogen evolution on MoS_2 is expected to occur predominantly at the M-edge (ΔG_H= 0.08 eV) rather than S-

edge (ΔG_H= 0.18 eV) [18]. With respect to WGS reaction, there have been disagreements on mechanism over MoS_2 catalyst. Some researchers attribute formate species to spectator (formed by a side reaction between CO_2 and H) and claim that both M- and S-edge sites follow a redox mechanism of successive surface oxidation by H_2O and reduction by CO [19, 20]; others correlate the formate to a favorable intermediate (formed via CO reaction with OH) on both edges of MoS_2 and thus propose a double mechanism through redox and associative paths [21]. However, even the widely accepted redox mechanism that supports the $MoS_{2-x}O_x$ site as active center does not allow to understand why sulfide catalysts would exhibit poor stability under H_2S-free condition, which is often interpreted as poor anti-oxidation capability for the formation of oxy-sulfide phase during the WGS reaction. On the contrary, the catalytic performance and stability would be significantly enhanced in H_2S-containing atmosphere [22, 23]. These highly divergent results indicate that redox mechanism is not well understood, especially for the role of $MoS_{2-x}O_x$ sites. Furthermore, the role of the support also requires special consideration [24]. On one hand, CO adsorbed on sulfide sites could spill over to the support [25], implying that the support could be involved in catalytic reaction whereas only sulfide phase is considered in DFT calculation; on the other hand, the interaction between the sulfide phase and the support results in varying the proportion of M-edge to S-edge sites [26], also affecting the catalytic activity [22]. Therefore, a direct observation of the catalytic performance of specific sites is required to get insight into the reactivity of M-/S-edge site.

The crucial issue in the surface reaction investigation on MoS_2 is how to readily identify and quantify each type of edge sites. In general, visual observation of morphology can be directly achieved by electron microscopy to qualitatively distinguish the two exposed edges. However, active metal dispersion as measured by microscopy is limited by statistical information. Fourier transform infrared (FTIR) spectroscopy coupled with probe molecules appears to be a powerful method by monitoring with the sufficient sensitivity the probe-surface interaction. In particular, all aspects of the catalyst system in

terms of the sulfide/support surface, titration of active edge sites, and electron transfer can be probed by CO adsorption at liquid nitrogen temperature followed by IR spectroscopy (CO/IR) [27-30]. Meanwhile, CO can also represent the realistic active site information being a reactant in WGS reaction.

In this work, two kinds of MoS_2/Al_2O_3 catalysts have been prepared with/or without citric acid through wetness impregnation method in order to obtain two morphologies of MoS_2 slabs with different proportion of M-edge to S-edge sites [4]. Next, the reactivity of each type of edge sites towards H_2O and/or CO is studied using CO/IR spectroscopy technique. Then, the stepwise WGS surface reaction is carried out to elucidate the mechanism routes. Finally, *operando* study coupling IR analysis of the catalyst surface and IR/GC analysis of the gas phase confirms the routes through *operando* identification of relevant long-lived intermediates. This work is the first to explore the effect of H_2O and CO on both M-edge and S-edge sites, allowing to identify the real active center of sulfide catalyst and to reveal the mechanism of WGS reaction. More importantly, understanding the reactivity of the M/S-edge sites with H_2O and CO also contributes to the design of sulfide catalysts for other reactions involving H_2O dissociation and CO conversion.

2. Experimental Section

2.1. Catalyst preparation

Mo/Al_2O_3 catalyst was prepared by wetness impregnation method using ammonium heptamolybdate tetrahydrated salt as molybdenum precursor ($(NH_4)_6Mo_7O_{24}\cdot 4H_2O$, MERCK). The supports, γ-Al_2O_3 (245 m^2/g, Sasol), were crushed and sieved into 0.2-0.5 μm fraction and then pre-calcined at 773K during 4h. The loading of Mo was targeted at a sub monolayer with 3 atoms Mo/nm^2. In addition, $Mo(CA=2)/Al_2O_3$ catalyst was prepared by same method but with citric acid (CA, $C_6H_8O_7\cdot H_2O$, PROLABO) as a chelating agent and the molar ratio of citric acid to Mo was kept at 2. After impregnation, the catalysts were left for maturation at ambient for 2h and then dried at 383K (1K/min)

during 16h. Note that the catalysts were not calcined in order to keep the chelating agent in its initial form. Mo/SiO_2 catalyst was prepared with same method than Mo/Al_2O_3 on SiO_2 (506 m^2/g, Merk).

2.2. Catalyst sulfidation

Catalyst sulfidation were performed *in situ* in a quartz glass IR cell. Sample was firstly grounded and pressed into a self-supporting pellet of ~20 mg and area of 2 cm^2 (precisely weighted). The pellet was then introduced into the glass cell and the cell was evacuated to ~1.0 $\times 10^{-6}$ torr to remove the air and physisorbed water. Afterward, the pellet was activated at atmospheric pressure at 723K in a flow of 30 ml/min 10% H_2S/H_2. At the end of activation at 723K for 2h, the IR cell was flushed under Ar flow, then evacuated during 1h at 723K and finally cooled down to room temperature under vacuum.

2.3. Low-temperature CO adsorption followed by IR spectroscopy (CO/IR)

After sulfidation, the pressure in the cell is around ~1.0 $\times 10^{-6}$ torr. Then the pellet was cooled down by liquid nitrogen to 100K for CO adsorption. Small calibrated doses of CO were introduced in the IR cell up to an equilibrium pressure of 133 Pa. IR spectra of adsorbed CO were recorded with a Nicolet iS50 FTIR spectrometer equipped with a MCT detector with 256 scans and a resolution of 4 cm^{-1}. For comparison, all the spectra presented were normalized to a sulfided catalyst pellet of 5 $mg.cm^{-2}$. The SI give the procedure for treatment after the sulfidation (SI1). The spectra treatment and subsequent calculation are also described in SI2.

2.4. Activity test

Before WGS reaction test, the as prepared catalyst was sulfided at 723K (3K/min) and 0.1MPa for 2h under a 30 ml/min flow of 10% H_2S/H_2. Then WGS reaction was carried out in a glass differential reactor under 0.5% CO and 1% H_2O in Ar balance with GHSV~ 9000 h^{-1} at 573K and 0.1MPa. The vapor of water was introduced into the system using a saturator with Ar as carrier gas. The water vapor pressure was controlled through a temperature tank set at 17.6°C (20 mbar). The pipelines were heated at 50°C to avoid water condensation. The outlet gas was analyzed by Varian 450 gas chromatograph

126 equipped with a PoraPlot Q column (Varian, 25 m, 0.53 mm, 20 μm) and thermal conductivity (TCD)
127 detector. The catalytic activity was expressed by the conversion of CO. Stepwise test experiments were
128 also performed in glass differential reactor under flow of pure CO or pure H_2O flow (completed by Ar).

129 **2.5. Operando IR/GC experiment**

130 The operando experiments have been performed in a Nicolet 6700 FTIR spectrometer equipped with a
131 specific IR-reactor cell, named IR "sandwich" cell. IR spectra of catalysts were directly recorded by
132 FTIR spectrometer equipped with a MCT detector using 64 scans and a resolution of 4 cm^{-1}.
133 Downstream the IR-reactor cell, the exhaust gases were analyzed simultaneously using an online IR-gas
134 cell and a GC equipped with TCD detector. Catalyst sulfidation were performed *in situ* in the IR-reactor
135 cell reactor. Sample was firstly grounded and pressed into a self-supporting pellet of ~15 mg and area of
136 2 cm^2. The pellet was then installed into the IR-reactor cell. Catalyst sulfidation were performed *in situ*
137 at atmospheric pressure under a flow of 30 ml/min 10% H_2S/H_2 at 723K. Finally, the reactor was cooled
138 down to 573K under pure Ar flow. Afterwards, WGS reaction was carried out under a 10 ml/min feed
139 flow of 0.5% CO and 1% H_2O in Ar balance.

140 **3. Results and Discussion**

141 **3.1. S-edge sites of MoS_2/Al_2O_3 catalysts are not sensitive to water treatment**

142 The reactivity with water of M-edge and S-edge sites of MoS_2 catalysts were evaluated on sulfided
143 Mo/Al_2O_3 and $Mo(CA=2)/Al_2O_3$ catalysts. CO adsorption (SI1) and HAADF-STEM study [31] have
144 previously demonstrated that the introduction of CA in the impregnation solution leads to higher S-/M-
145 edge ratio with a small decrease in total edge sites (reference J phys chem C jianjun to add). Then, the
146 catalysts were characterized by CO/IR at around 100 K without any air contact after (i) in-situ
147 sulfidation at 723 K, (ii) subsequent treatment under pure $H_2{}^{18}O$ vapor at 573 K and (iii) subsequent
148 treatment under 10% H_2S/H_2 at 723K i. e. resulfidation (Figure 1).

For both Mo/Al_2O_3 and $Mo(CA=2)/Al_2O_3$ catalysts, the CO uptake on M-edge sites (band at ~2112 cm^{-1}) decreases significantly after water treatment. This is in agreement with previous study and ascribed to an exchange reaction of sulfur-oxygen on the M-edge, making the oxygen-substituted MoS_2 sites unfavorable for CO adsorption [32]. Figure 1a and b show that this S/O exchange on M-edge sites is not reversible under 10% H_2S/H_2 treatment indicating the good stability of the formed $Mo(S_xO_y)_{zc}$ sites. This notation is chosen to indicate some O in the coordination environment of Mo edge site without indication of the coordination number nor the proportion of S/O exchange.

On Mo/Al_2O_3, the intensity of the *v*(CO/S-edge) band at 2064 cm^{-1} appears unaffected by water treatment whereas an increase of the CO/S-edge band area is observed with a downward shift on $Mo(CA=2)/Al_2O_3$. Moreover, the water effect on S-edge of $Mo(CA=2)/Al_2O_3$ catalyst is reversible after the 10% H_2S/H_2 treatment and thus seems to be similar to those observed when sulfur vacancies are created during hydrogen post-treatment (SI2). The creation of vacancies could be related to H_2 production during the treatment with H_2O of $Mo(CA=2)/Al_2O_3$. The surface IR spectrum reveals that carbonaceous residues are present after sulfidation of the catalyst prepared with CA, resulting in bands ranging from 1700 to 1400 cm^{-1} (SI3 a). After $H_2{}^{18}O$ treatment at 573K, discernable changes in the complex signal of the carbonaceous residues are observed. Interestingly, carbon dioxide labeled by isotope ^{18}O is formed in the gas phase (SI3 b). Thus, $H_2{}^{18}O$ is reduced by the residual carbonaceous species and as a consequence, the formation of carbon dioxide should be accompanied by the formation of H_2 (undetectable on IR spectra). Specific formation of H_2 upon H_2O feed on this catalyst will be further confirmed in the stepwise tests described later on.

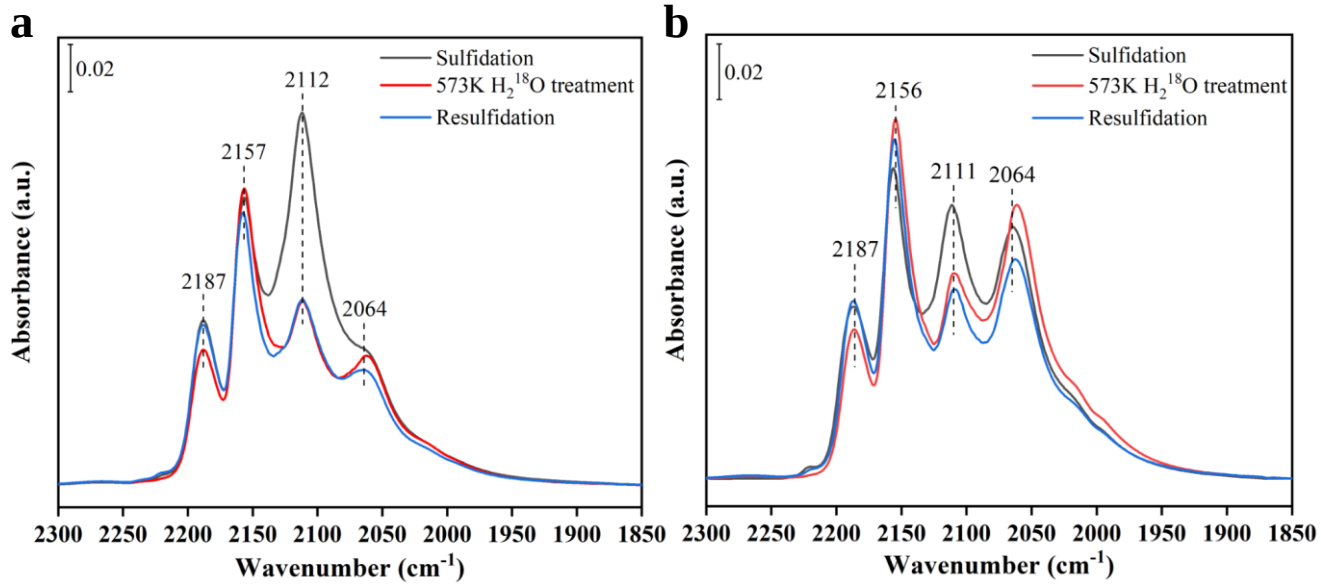

Figure 1. Investigation of the effect of water ($H_2{}^{18}O$) treatment on M-edge and S-edge sites. IR spectra of CO adsorption at 133 Pa equilibrium on sulfided Mo/Al_2O_3 (a) and $Mo(CA=2)/Al_2O_3$ (b) catalysts after sulfidation, water treatment ($H_2{}^{18}O$, 600 Pa and 573K) and subsequent resulfidation.

Finally, on $Mo(CA=2)/Al_2O_3$, the intensity of the ν(CO/S-edge) band after the resulfidation treatment is lower than that after the initial sulfidation. In parallel, it has been verified that in absence of water treatment, resulfidation does not affect the amount of detected S-edge sites (SI4 a). Thus, water treatment also leads to some irreversible changes of S-edge sites that could be ascribed to some S/O exchanges during water treatment, in the same way as for the M-edge.

In conclusion, two features can occur during water treatment whose extent depend on the sulfide slab edges: *(i)* S/O exchange that occurs more easily on M-edge site than on S-edge. *(ii)* sulfur vacancies creation that occurs only on S-edge and only on catalyst presenting carbonaceous residues.

3.2. S-edge sites of MoS_2/Al_2O_3 catalysts form vacancy upon CO treatment

The effect of CO treatment (40%^{13}CO/60%^{12}CO at 573K) on edge sites of sulfided catalysts was probed by CO/IR (^{12}CO at 100K) with a similar strategy than for water treatment. After Mo/Al_2O_3 and $Mo(CA=2)/Al_2O_3$ catalysts were treated with ^{13}CO/^{12}CO at 573K, the CO uptake on the S-edge

increases significantly, while the CO adsorption at the M-edge is almost unchanged (Figure 2, Table 1). Moreover, the *ν*(CO/S-edge) frequency undergoes a slight shift towards lower wavenumber after CO treatment in accordance with the formation of sulfur vacancy. In addition, resulfidation after CO treatment was carried out on Mo(CA=2)/Al_2O_3 and the spectrum of CO adsorption (SI6 b) clearly show that the initial edge state is totally recovered.

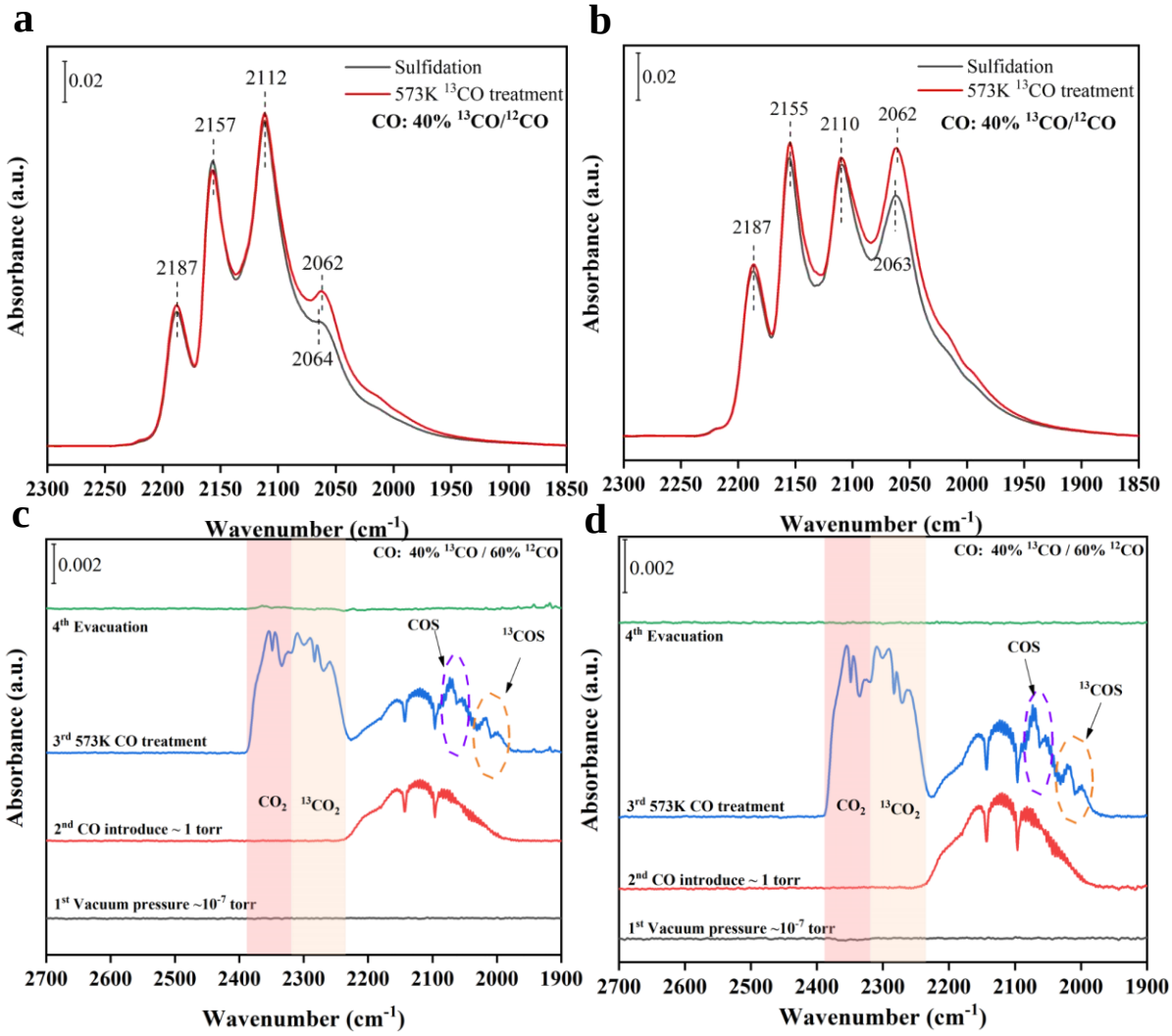

Figure 2. Investigation of the effect of CO treatment on M-edge and S-edge sites. a, b, IR spectra of CO adsorption at 133 Pa equilibrium before and after CO treatment on sulfided Mo/Al_2O_3 catalyst (a) and Mo(CA=2)/Al_2O_3 catalyst (b). c, d, In-situ IR spectra of gas phase recorded during CO treatment on sulfided Mo/Al_2O_3 catalyst (c) and Mo(CA=2)/Al_2O_3 catalyst (d).

The IR spectra recorded during the CO treatment show the formation of $^{13}COS/^{12}COS$ in the gas phase (Figure 2c and d). These results evidence that CO treatment leads to sulfur vacancy creation through oxidation of CO into COS. Figure 2a and b points out that S-edge site is more reactive towards CO treatment than M-edge site. Interestingly, the signal of carbon dioxide was also clearly detected in gas phase during CO treatment. This could be ascribed to COS hydrolysis on hydroxyl group of support, or direct reaction of CO with OH group of the support. In order to check the direct reaction between CO and OH groups, CO treatment was conducted on pure alumina (Figure 3).

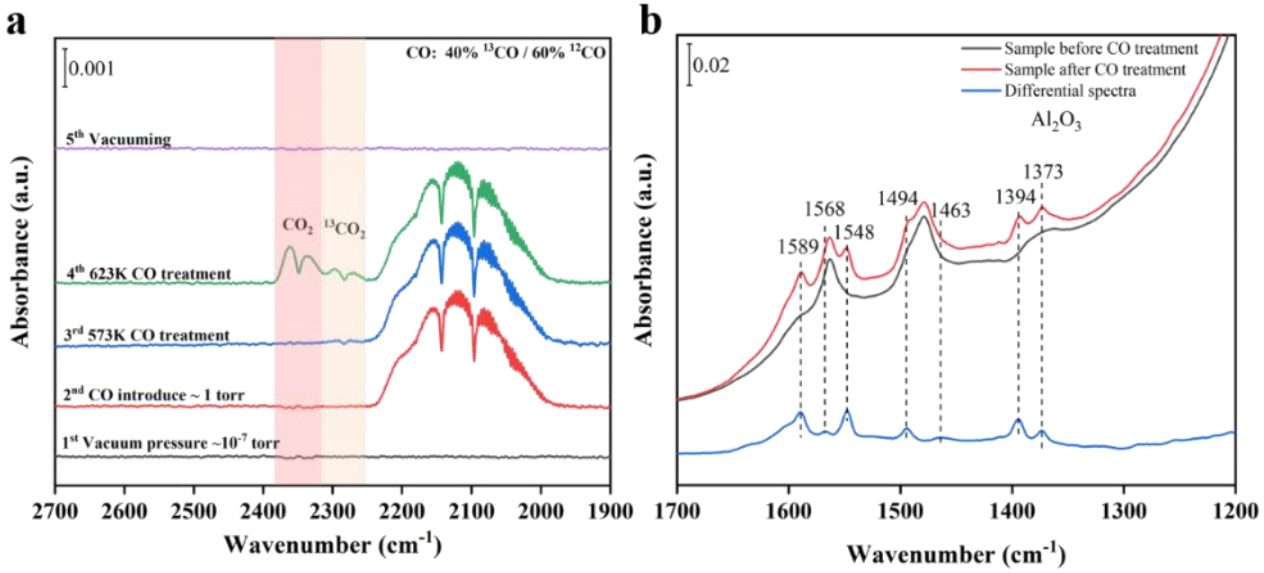

Figure 3. CO treatment on pure Al_2O_3. a, *In-situ* IR spectra of gas phase recorded during CO treatment on Al_2O_3. **b,** IR spectra of Al_2O_3 recorded before and after CO treatment (CO treatment: 133 Pa 40%^{13}CO/60%^{12}CO, 623K/2h).

The starting temperature of CO_2 formation on pure Al_2O_3 is 623K, i.e. a higher temperature than on Mo/Al_2O_3. Thus, OH groups of alumina are not active on their own at 573K. However, we cannot exclude that the presence of sulfide phase enhances the reactivity of CO with OH groups through adsorbing and/or activating CO on sulfide site and subsequently spilling it over to the support. Moreover, comparing the IR spectra of Al_2O_3 before and after CO treatment at 623K, it can be found

211 that a small amount of formate species (1589, 1394 and 1373cm^{-1}) and carbonate species (1548 and
212 1494 cm^{-1}) was accumulated on the surface of Al_2O_3. Formate are also observed after CO treatment at
213 573K on Mo/Al_2O_3 (SI5). However, as described above, formate species could be involved in CO_2
214 production as active species or be only present as spectator ones. To check this point, the stability of
215 formate species was studied. As shown in Figure S6, formate species on Mo/Al_2O_3 decompose into CO_2
216 starting from 573 K. These results show that both the sulfide sites and OH groups are involved in the
217 indirect or direct CO_2 formation on Mo/Al_2O_3.
218

219 **Table 1**: Concentration of edge sites on Mo/Al_2O_3 and $Mo(CA=2)/Al_2O_3$ catalysts after sulfidation and
220 CO treatment detected by CO/IR spectra.

Catalyst	edge	Sulfidation		573K CO	
		v(CO) (cm^{-1})	n (μmol g^{-1})	*v*(CO) (cm^{-1})	n (μmol g^{-1})
Mo/Al_2O_3	M	2112	59	2112	60
	S	2064	19	2062	25
$Mo(CA=2)/Al_2O_3$	M	2110	38	2110	39
	S	2063	31	2062	37

221

222 **3.3. S/O exchanged sites are not involved in the redox pathway of WGS on MoS_2/Al_2O_3**
223 **catalysts**

224 As mentioned above, because the M-edge site is prone to the S/O exchange reaction, it is most likely
225 to follow the conventional redox route, with the $Mo(S_xO_y)_{zc}$ site as the active center. In order to examine
226 the reactivity of $Mo(S_xO_y)_{zc}$ sites toward CO, CO/IR was performed stepwise after successive H_2O
227 treatment, resulfidation and CO treatment at 573 K on sulfided Mo/Al_2O_3 catalyst. As shown in Figure

4a, the water treatment leads to S-O exchange reaction mainly at M-edge and formation of the $Mo(S_xO_y)_{zc}$ sites. Following H_2O treatment, we have seen that the $Mo(S_xO_y)_{zc}$ on M-edge after resulfidation is not modified, but also subsequent CO treatment show no effect on the CO adsorption on M-edge site. In addition, the direct CO treatment after water treatment was also performed on sulfided Mo/Al_2O_3 catalyst (SI7) and the CO uptake of M-edge after H_2O + CO + resulfidation is the same as that obtained after water treatment, indicating that no $Mo(S_xO_y)_{zc}$ site is reduced by CO. Thus, the formation of oxygen vacancy by CO on $Mo(S_xO_y)_{zc}$ sites of M-edge can be discarded. Note that the CO uptake on the S-edge increases slightly after CO treatment, this could be attributed to the reaction between CO and MoS_2 site to create sulfur vacancy, as evidenced by the gas phase analysis which reveals the formation of COS (Figure 4b). As previously, CO_2 ($C^{16}O_2 + C^{18}O^{16}O$) is also detected (Figure 4b) but the CO_2/CO ratio is greater than for CO treatment performed directly after sulfidation (Figure 2). This could be ascribed to the enhanced COS hydrolysis and CO reactivity with hydroxyl group on the hydrated support. Indeed, formate species (Figure 4c) are observed on the catalyst surface.

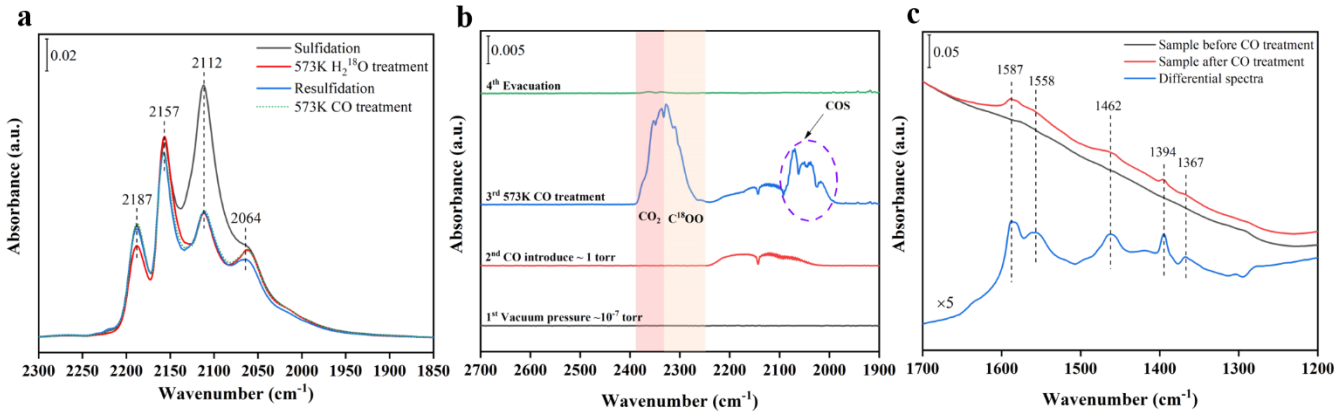

Figure 4. Subsequent CO treatment on water treated sulfided Mo/Al_2O_3 catalyst. a, CO/IR spectra recorded at 133 Pa equilibrium after sulfidation, water treatment, resulfidation, and subsequent CO treatment. b, *in situ* IR spectra of gas phase recorded during CO treatment. c, IR spectra of catalyst surface recorded before and after CO treatment in a.

3.4. The support also has a role in WGS pathway

In order to discriminate between the two possible pathways to form CO_2 from CO, i.e. COS hydrolysis pathway or formate pathway, similar study has been performed on Mo/SiO_2. Indeed, on Mo/SiO_2, no formate is expected to be formed on the support. Meanwhile, its sulfide phase is known to have preferentially S-edge sites exposed as confirmed by Figure 5a [26]. From the spectrum after sulfidation, the concentration of sites is calculated to be 17 $\mu mol.g^{-1}$ for S-edge and 33 $\mu mol.g^{-1}$ for M-edge.

As shown in Figure 5a and c, CO (40%^{13}CO/60%^{12}CO) treatment of sulfided Mo/SiO_2 leads to the formation of vacancies mainly on S-edge along with the formation of carbonyl sulfide and carbon dioxide. This is consistent with results on Al_2O_3-supported Mo catalysts. However, on Mo/SiO_2, the carbon dioxide should be formed through the carbonyl sulfide pathway since formate intermediates are, as expected, not detected (Figure 5b: no OH consumption, no formate formation). Water treatment of sulfided Mo/SiO_2 has similar effect as on Mo/Al_2O_3 (Figure 5d), that is to say: almost no effect on S-edge site amount and strong decrease of M-edge sites. Similarly, subsequent CO treatment creates vacancy on both edges but mainly on S-edge. Meanwhile, COS and CO_2 are observed in gas phase in accordance with sulfur vacancy formation. Note that contrary to Mo/Al_2O_3, the proportion of CO_2 to CO formed on Mo/SiO_2 when the CO treatment is performed after the water one, is not greater than for direct CO treatment just after sulfidation. This is in accordance with the absence of direct reaction between SiOH and CO. Finally, resulfidation does not allow to reach back the initial sulfide site amount especially on M-edge and the corresponding CO uptake of M-edge is very similar to that measured after only water treatment. These results are totally in agreement with the ones obtained on Mo/Al_2O_3.

One difference between Mo/SiO_2 and Mo/Al_2O_3 catalysts concerns the effect of H_2O treatment on S-edge sites. Indeed, even if S-edge sites are preferential sites of sulfide slabs on Mo/SiO_2, no increase in

S-edge sites is observed after water treatment in contrary to the case of Mo(CA=2)/Al_2O_3 (Figure 1b). This difference is related to the presence or absence of citric acid residues. As discussed in previous section, these species can react with water leading to some H_2 production and then formation of sulfur vacancies at S-edge. Hence, the involvement of carbonaceous residue proposed previously is confirmed by the absence of S-edge vacancy creation upon H_2O treatment on Mo/SiO_2.

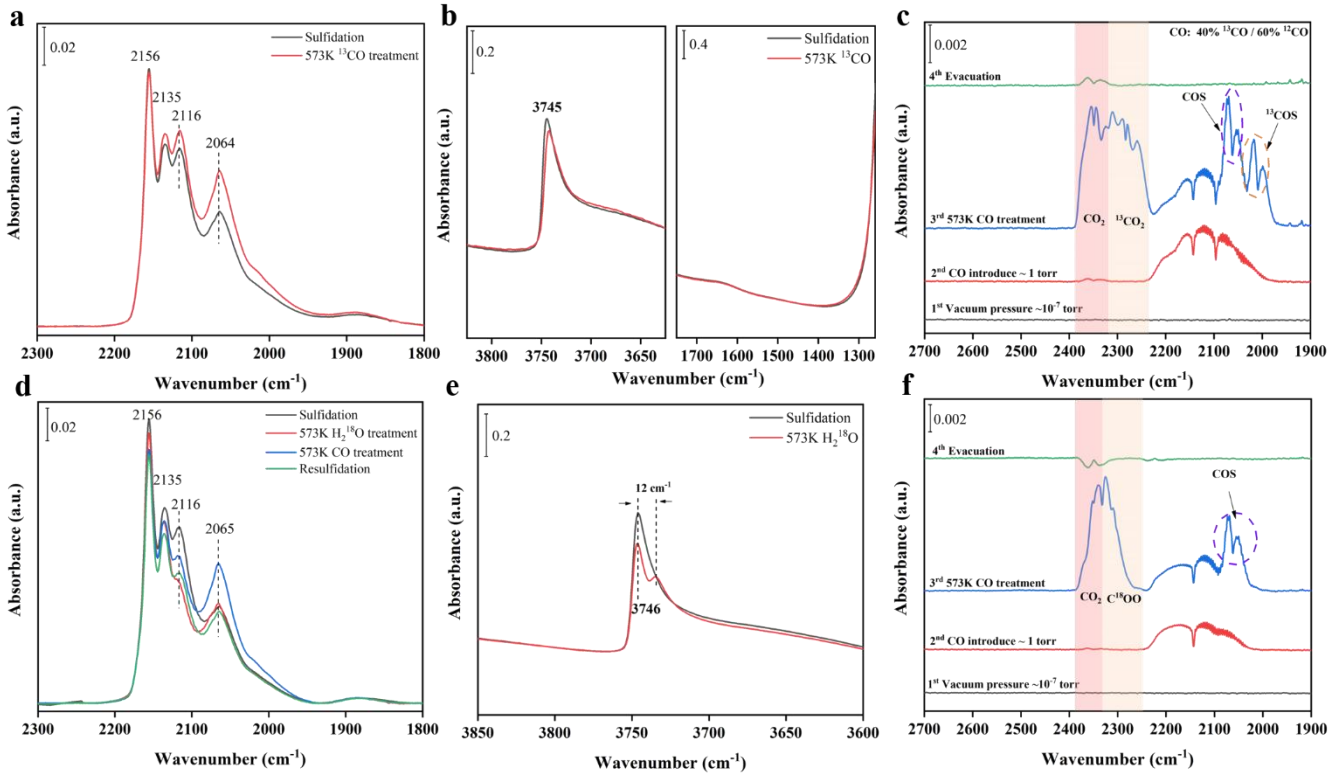

Figure 5. H_2O or/and CO treatment on sulfided Mo/SiO_2 catalysts. a, CO/IR spectra of the Mo/SiO_2 catalyst after sulfidation and subsequent CO treatment. b, IR spectra of Mo/SiO_2 recorded before and after CO treatment in a. c, *in situ* IR spectra of gas phase recorded during CO treatment. d, IR spectra of CO adsorption at 133 Pa equilibrium on Mo/SiO_2 catalyst after sulfidation, H_2O treatment, CO treatment and resulfidation. e, IR spectra of Mo/SiO_2 recorded before and after $H_2{}^{18}O$ treatment in d. f, *in situ* IR spectra of gas phase recorded during CO treatment on sulfided Mo/SiO_2 pretreated by $H_2{}^{18}O$.

3.5. WGS activity

WGS performances were evaluated for Mo/Al_2O_3, $Mo(CA=2)/Al_2O_3$ and Mo/SiO_2 catalysts under 0.5% CO and 1% H_2O in Ar balance with GHSV~ 9000 h^{-1} at 573K (Figure 6). The two alumina-supported catalysts present a very strong deactivation up to 4 hours of time-on-stream (TOS). Then, the activity of Mo/Al_2O_3 catalyst continues to slightly decrease while the activity of $Mo(CA=2)/Al_2O_3$ catalyst remains stable. Finally, sulfided $Mo(CA=2)/Al_2O_3$ catalyst exhibits a higher activity than Mo/Al_2O_3 catalyst at high TOS. As for Mo/SiO_2 catalyst, it displays some deactivation up to 2 hours of TOS, and then presents a stable conversion. However, the activity of Mo/SiO_2 catalyst is lower than those of the alumina-supported catalysts whatever the TOS. Taking into account the complexity in terms of the continuous change in M-edge site environments and the role of the interface between support and sulfide sites, the intrinsic activity of the two edge sites is not possible to be determined from the initial site characterization. However, the different responses of the two edges to H_2O and CO means that they follow different reaction pathways.

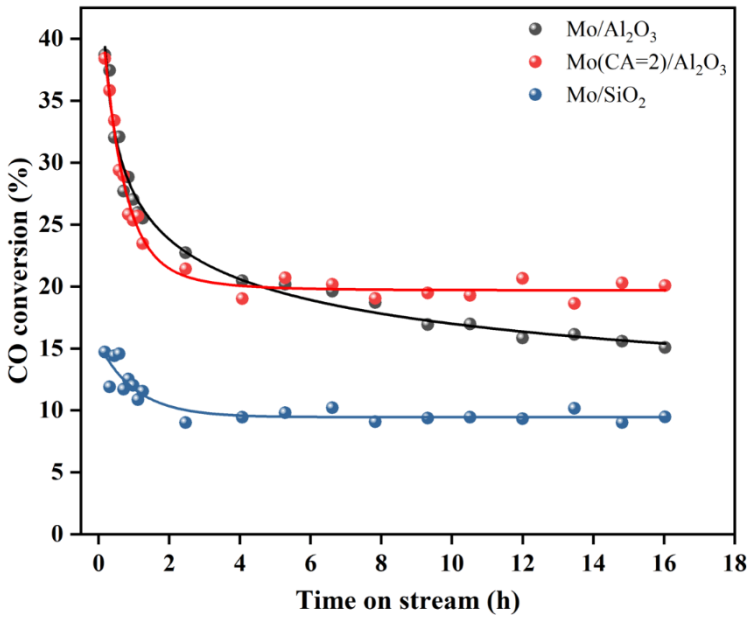

Figure 6. WGS reaction vs TOS. CO conversion over Mo/Al_2O_3, $Mo(CA=2)/Al_2O_3$ and Mo/SiO_2 catalysts during WGS reaction (feed gas: 0.5% CO and 1% H_2O in Ar balance at GHSV= 9000 h-1 and Tr = 573K).

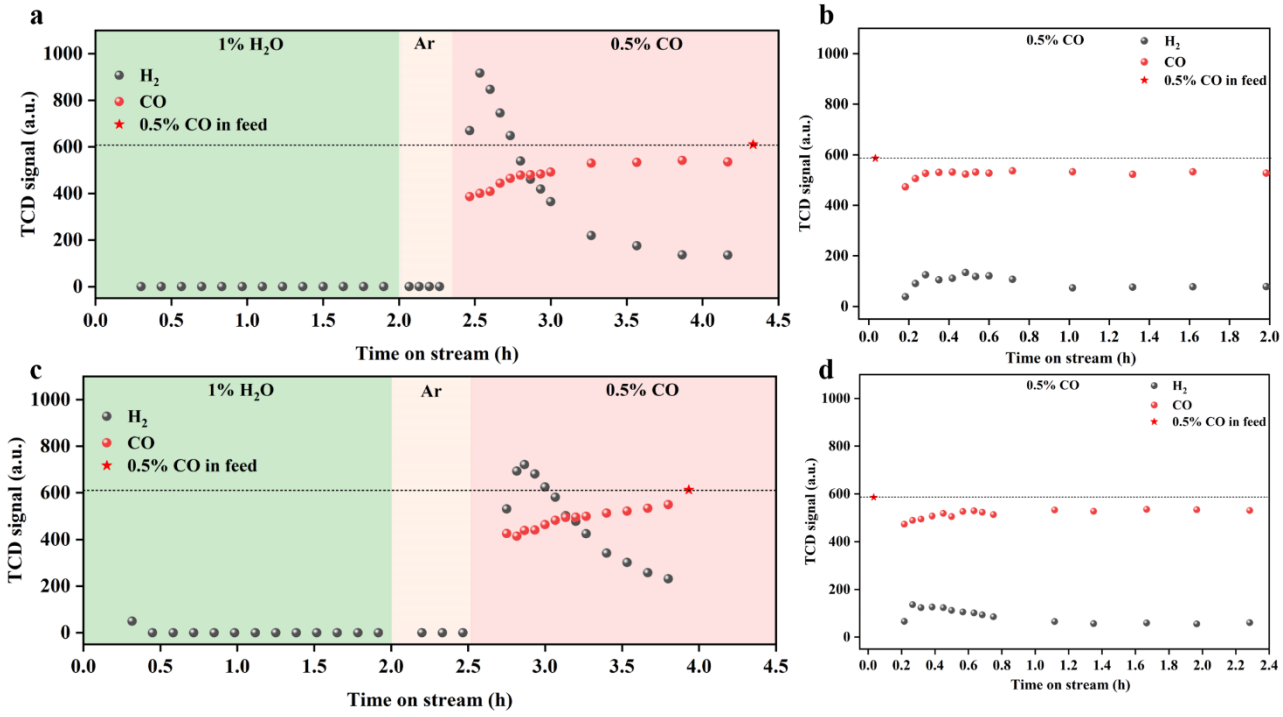

Figure 7. Stepwise WGS reaction. a, c, Water feed followed by CO feed at 573K over sulfided Mo/Al_2O_3 (a) and $Mo(CA=2)/Al_2O_3$ (b). b, d, CO feed at 573K on Mo/Al_2O_3 (b) and $Mo(CA=2)/Al_2O_3$ (d).

Stepwise WGS reaction experiments were performed on the Al_2O_3 supported catalysts to check if the oxidation/reduction pathway was occurring (Figure 7). After sulfidation of Mo/Al_2O_3 catalyst, if only H_2O is flowing at 573 K (without CO in the flow), no H_2 signal is detected (Figure 7a). Similar behavior is observed for the sulfided $Mo(CA=2)/Al_2O_3$ catalyst, although a limited amount of H_2 is released at the beginning of the alone water feed (Figure 7c). As previously discussed, this small H_2 production comes from the reaction of water with residual carbonaceous species. Thus, the direct oxidation step by H_2O giving H_2 can be discarded. For both catalysts, if CO is introduced alone at 573 K after the H_2O flow, a high amount of H_2 is released and then H_2 formation reaches a much lower plateau. If now CO alone was introduced firstly after sulfidation (Figure 7b and d), a small production of H_2 occurs that is stable with TOS, and close to the plateau obtained in the previous experiment for long TOS (Figure 7a and c). Under CO alone flow, H can only come from the catalyst surface either as OH or SH species. In

particular, knowing that OH species can be involved in both COS hydrolysis and formate formation, they can react directly (formate path) or indirectly with CO (COS path).

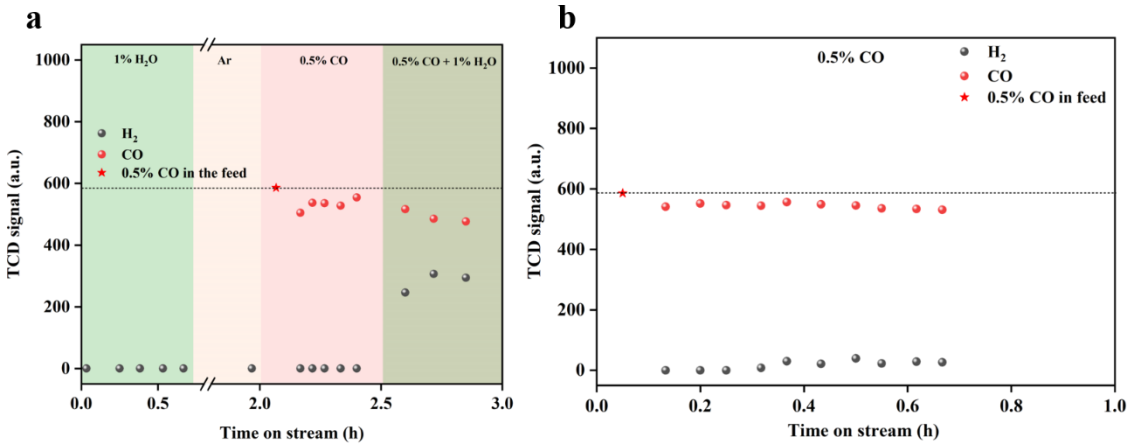

Figure 8. Stepwise WGS reaction on sulfided Mo/SiO_2. a, Water feed followed by CO feed at 573K and finally followed by WGS reaction. b, CO feed at 573K.

Similar study was performed on Mo/SiO_2 (Figure 8). If CO is firstly introduced alone, H_2 production is almost undetectable (Figure 8b). Moreover, on this catalyst, the conversion of CO and formation of H_2 are not favored by the H_2O pre-treatment. As shown in Figure 8a, water in the feed is necessary to produce H_2 on Mo/SiO_2. These results confirm that SiOH are not involved in the reaction pathway.

The WGS reaction was further studied by *operando* IR/GC experiments that combined IR analysis of the surface species of the catalyst and on-line analysis by GC and gas phase IR of the reaction products (Figure 9). For the three catalysts, the conversion is in the same range than in the differential reactor although not totally the same. However, the same tendencies are observed as in terms of stability with TOS. Indeed, alumina-supported catalysts present a marked deactivation (up to ~0.5 h) that is not observed on silica-supported catalyst (Figure 9a). Moreover, alumina-supported catalyst is more stable when prepared with citric acid. After stabilization, the conversion is comprised between 15 to 10% for the three catalysts.

Meanwhile, the IR spectra of the Mo/Al_2O_3 show after a few minutes of reaction the appearance of a band at 2910 cm^{-1} as well as bands at 1590 and the doublet at 1392 and 1377 cm^{-1} which show the formation of formate species (Figure 9b). After pure Ar flow purge (red spectrum), the signal of water in gas phase is eliminated which makes clearer the observation of the bands at 2910, 1590, 1392 and 1377 cm^{-1}. These are respectively assigned to $\nu(CH)$, $\nu(OCO)_{asym}$, $\delta(CH)$ and $\nu(OCO)_{sym}$ of formate species on the Mo/Al_2O_3 catalyst surface [33]. In parallel, the gas phase IR spectra reveals CO consumption and CO_2 formation as well as the formation of a limited amount of COS (Figure 9c).

On the IR spectra of $Mo(CA=2)/Al_2O_3$ catalyst, despite the presence of the complex massif due to carbonaceous residues, bands characterizing formate intermediate can be observed. As with Mo/Al_2O_3, CO consumption and CO_2 formation are also observed in the gas phase spectra. In addition, at the beginning of the reaction, larger COS amounts are released on this catalyst than on the catalyst without citric acid. However, the COS production decreases strongly and rapidly after the first TOS, and then COS signal stays relatively stable and at value close to Mo/Al_2O_3.

On Mo/SiO_2 catalyst, no formate species are formed in agreement with the previous IR observations. Meanwhile, gas phase IR spectra show CO consumption and CO_2 production as well as COS formation. In this case, the COS production decreases at beginning but more slightly than for the alumina-supported catalysts and then presents a stable value.

So in conclusion, WGS study performed in differential reactor and in the *operando* set up points out that (i) activity of WGS reaction on alumina-supported catalysts is higher than that on silica-supported catalyst; (ii) stability of WGS reaction decreases in the following order: $Mo/SiO_2 > Mo(CA=2)/Al_2O_3 > Mo/Al_2O_3$; (iii) formate intermediates are observed only on alumina-supported catalysts ; (iv) COS production occurs for all catalysts, but Mo/Al_2O_3 presents limited COS release throughout TOS; (v) for Mo/SiO2, the WGS activity should be linked only to the S-edge sites via the COS route.

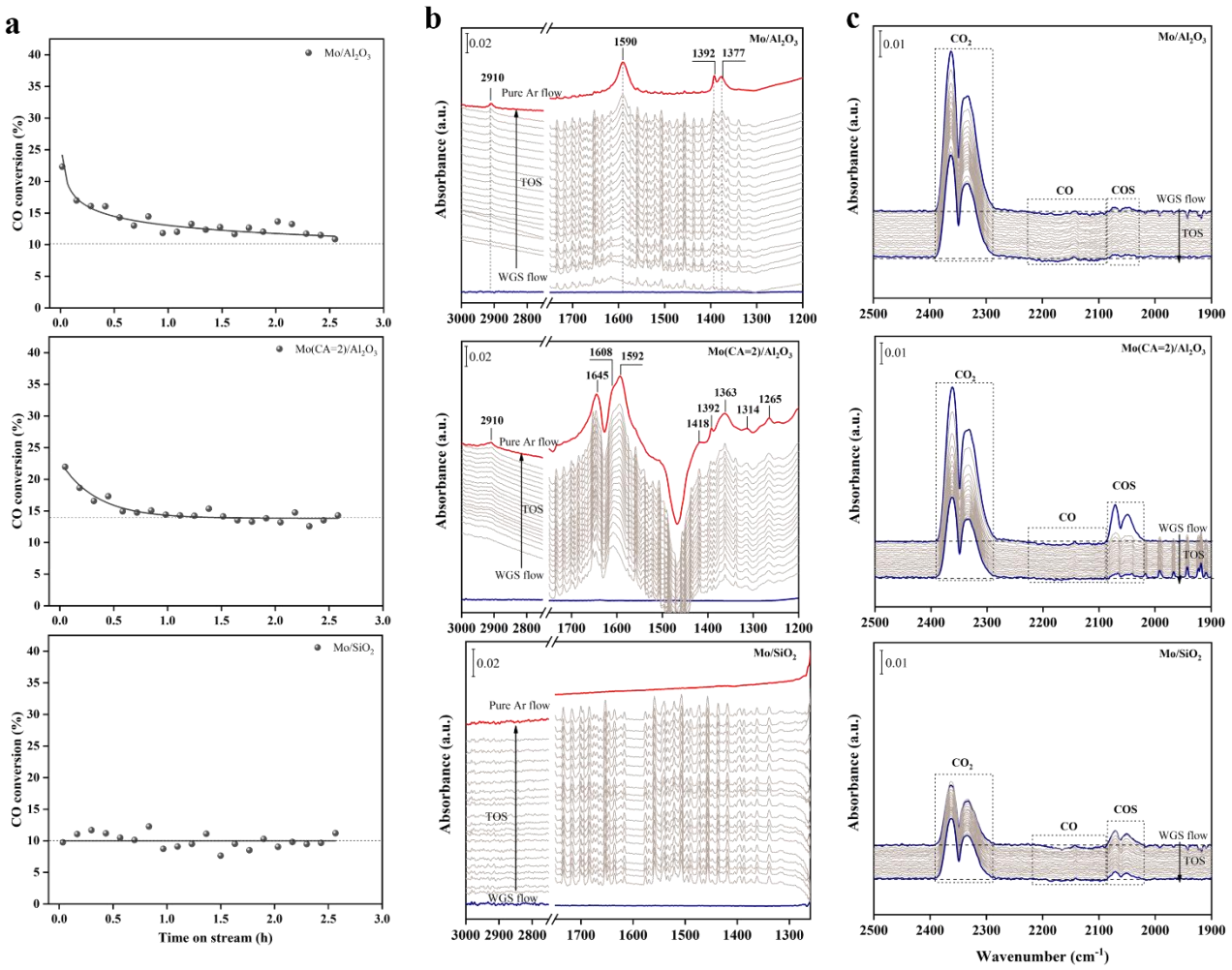

Figure 9. ***Operando*** **IR/GC study of sulfided Mo/Al_2O_3, $Mo(CA=2)/Al_2O_3$ and Mo/SiO_2 during WGS reaction at 573K versus TOS**. a, CO conversion. b, IR spectra of the catalysts during the WGS reaction (in grey) and after the reaction under Ar flow (in red) (All spectra correspond to catalyst spectra recorded at 573 K at given TOS minus catalyst spectrum recorded at 573 K prior the WGS flow). c, IR spectra of the gas phase during the WGS reaction (blue spectra correspond to that taken at the beginning and at the end of the reaction. All spectra correspond to gas phase spectra recorded at given TOS minus spectrum under the initial WGS feed flow)

3.6. New insights on WGS mechanisms on sulfide catalysts

Two mechanisms are usually considered for WGS reaction over sulfide catalysts, such as the associative mechanism and the redox mechanism [34]. In the associative mechanism, intermediate

formate species are formed on the catalyst surface via reaction of adsorbed CO with surface OH groups, which then decompose to CO_2 and H_2 [21]. For the case of the redox mechanism, the surface of catalyst is alternatively oxidized by water and then reduced by CO[12, 13].

Based (i) on the results of stepwise reactions and in particular on the production of H_2 under the CO alone feed, (ii) from the direct observation of formate intermediates in *operando* studies and (iii) the observed decomposition of formate at 573K on Mo/Al_2O_3, one can conclude that the formate mechanism occurs on Al_2O_3-supported MoS_2 catalysts at 573K. It must be underlined that at this temperature, WGS reaction does not occur on pure alumina, indicating that the vicinity between the Al-OH groups and the sulfide phase facilitates the formate species formation and thus play a role in the catalyst reactivity.

However, various observations point out that another reaction route exists. Indeed, silica-supported MoS_2 catalyst present a stable CO conversion whereas no formate species are formed during the WGS reaction. The conventional redox mechanism was firstly considered, in which the water-induced $Mo(S_xO_y)_{zc}$ site is proposed as the active center and then reduced by CO to produce CO_2 and give rise to a vacancy site [12, 13]. However, the CO/IR studies (Figure 4) vividly demonstrate that this oxygen substituted $Mo(S_xO_y)_{zc}$ site formed in situ by water treatment is stable toward CO treatment, thus preventing a direct redox process. In addition, this $Mo(S_xO_y)_{zc}$ site also shows excellent stability even in 10% H_2S/H_2 treatment and thus cannot be re-sulfided back to the initial state. These results suggest that the proposition of the conventional redox mechanism associated with $Mo(S_xO_y)_{zc}$ site might not be correct, and this water-induced S/O exchange reaction is an irreversible poisoning process for MoS_2, especially for M-edge site.

The IR gas phase spectra collected during the WGS reaction substantiate the formation of COS production. Thus, a novel redox mechanism associated with COS route can be proposed (equation 1-3). In this three-stage novel mechanism, the catalyst surface is firstly reduced by CO to form COS, then

393 COS is hydrolyzed to give rise to CO_2 and H_2S, and finally the sulfur vacancy can be refilled by H_2S to
394 returns back to its pre-reaction surface state:

395 $$CO + MoS_2 \rightarrow MoS\Delta + COS \quad (1)$$

396 $$COS + H_2O \rightarrow CO_2 + H_2S \quad (2)$$

397 $$H_2S + MoS\Delta \rightarrow MoS_2 + H_2 \quad (3)$$

398 This proposal is consistent with both γ-Al_2O_3 and sulfide phase known as commercial COS hydrolysis
399 catalysts [35, 36], and MoS_2 catalyst recognized as a good candidate for H_2S decomposition to yield H_2
400 [37]. In addition, under the regime of the COS hydrolysis pathway during WGS reaction, the
401 unconverted COS inevitably leads to sulfur loss, which also well explains why addition of H_2S in the
402 feed leads to a high and stable catalytic performance [5, 22].

403 Interestingly, Table 1 shows that CO forms vacancies on S-edge, and not on M-edge. Hence, this
404 novel redox mechanism involving COS can be exclusively ascribed to the S-edge sites. Note that one
405 cannot exclude that the formate route may also happen on the S-edge of alumina-supported catalysts. On
406 contrary, the activity of M-edge sites in WGS is only ascribed to the formate mechanism. Consequently,
407 on Mo/SiO_2, these M-edge sites should not be involved in reaction and CO conversion is entirely due to
408 the contribution of the COS pathway at S-edge. Knowing that the M-edge sites are irreversibly sensitive
409 to water, the deactivation with TOS observed on Al_2O_3 supported catalysts and more strongly on
410 Mo/Al_2O_3 having lower S/M edge ratio (Figure 6) can then be ascribed to these M-edge sites.

411 Hence, on Al_2O_3-supported MoS_2 catalysts, both formate and COS redox reaction routes occur
412 preferentially on M- and S-edge sites, respectively (Figure 10). As a general conclusion, the nature of
413 the support and the S-/M-edge ratio of the sulfide slabs determine the mechanisms and the stability of
414 the WGS reaction.

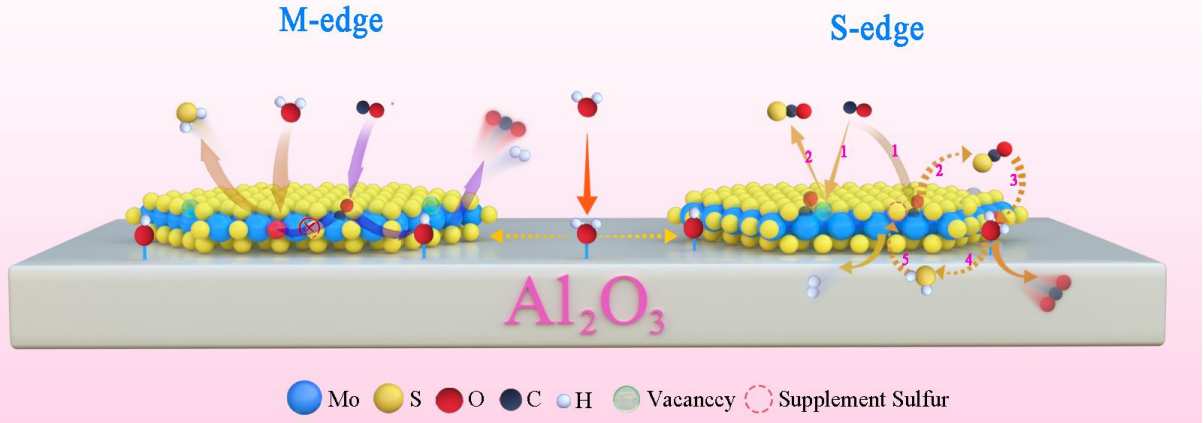

Figure 10: Schematic of reaction routes for WGS reaction over M-edge and S-edge sites of MoS_2 slab.

4. Conclusion

The effects of WGS reactants (H_2O, CO) on M-edge and the S-edge sites of MoS_2 catalysts were explored by *in situ* IR spectroscopy. IR/CO experiments demonstrated that the M-edge site is sensitive to water to form the oxygen-substituted $Mo(S_xO_y)_{zc}$ site via S/O exchange reaction, while the S-edge site is sensitive to CO to form vacancies and release COS. Stepwise reaction experiments and IR Operando study revealed that two different WGS pathways are involved in H_2 production on sulfide: *(i)* Hydrogen can be produced by WGS reaction following formate mechanism i.e. through the reaction of CO with hydroxyl group of alumina support; *(ii)* Hydrogen can also be produced by a redox mechanism. However, the conventional redox mechanism that occurs by direct oxidation by water and subsequent reduction by CO has to be excluded on the Mo-sulfide catalysts. Moreover, the stability of $Mo(S_xO_y)_{zc}$ species towards CO exclude their role as WGS active centers. However, the detection of COS formation during WGS reaction leads to propose a novel redox mechanism associated with this intermediate. Interestingly, the findings in different response of two edge site towards CO indicate that formate route occurs mainly on the M-edge, while the novel redox mechanism occurs exclusively on S-edge of the sulfide slabs. Finally, WGS tests show that the M-edge site is not a stable and durable active center compared with S-edge.

This work gives the direction for obtaining high stability sulfide catalyst for reactions involving water by improving stability of M-edge sites and also reveals that the active sites of CO activation and

435 oxidation are located at the S-edge, which also contributes to the design of sulfide catalysts for other
436 reaction, such as methanethiol synthesis.
437

Corresponding Author: * E-mail: laetitia.oliviero@ensicaen.fr

ORCID: Laetitia Oliviero: https://orcid.org/0000-0002-7931-439X

Author Contributions

The manuscript was written through contributions of all authors. All authors have given approval to the final version of the manuscript.

Funding Sources

W. Zhao is grateful for the MOPGA grant (Campus France MOPGA-927541K)

Acknowledgments

Alexandre Vimont, Philippe Bazin and Yoann Levaque from LCS are greatly acknowledged for the IR experiments and activity measurements for WGS reaction. The authors thank Jinxing Mi and Xiaoping Chen for kindly helping with Graphical abstract and Scheme design.

REFERENCES

[1] J. Kibsgaard, Z. Chen, B.N. Reinecke, T.F. Jaramillo, Engineering the surface structure of MoS_2 to preferentially expose active edge sites for electrocatalysis, Nat Mater, 11 (2012) 963-969.

[2] L. Liu, J. Wu, L. Wu, M. Ye, X. Liu, Q. Wang, S. Hou, P. Lu, L. Sun, J. Zheng, L. Xing, L. Gu, X. Jiang, L. Xie, L. Jiao, Phase-selective synthesis of 1T' MoS_2 monolayers and heterophase bilayers, Nat Mater, 17 (2018) 1108-1114.

[3] J. Hu, L. Yu, J. Deng, Y. Wang, K. Cheng, C. Ma, Q. Zhang, W. Wen, S. Yu, Y. Pan, J. Yang, H. Ma, F. Qi, Y. Wang, Y. Zheng, M. Chen, R. Huang, S. Zhang, Z. Zhao, J. Mao, X. Meng, Q. Ji, G.

Hou, X. Han, X. Bao, Y. Wang, D. Deng, Sulfur vacancy-rich MoS2 as a catalyst for the hydrogenation of CO_2 to methanol, Nature Catalysis, 4 (2021) 242-250.

[4] J. Chen, F. Maugé, J. El Fallah, L. Oliviero, IR spectroscopy evidence of MoS 2 morphology change by citric acid addition on MoS_2/Al_2O_3 catalysts – A step forward to differentiate the reactivity of M-edge and S-edge, J. Catal., 320 (2014) 170-179.

[5] T. Sasaki, T. Suzuki, H. Iizuka, M. Takaoka, Reaction mechanism analysis for molybdenum-based water-gas shift catalysts, Applied Catalysis A: General, 532 (2017) 105-110.

[6] B. Hinnemann, P.G. Moses, J. Bonde, K.P. Jorgensen, J.H. Nielsen, S. Horch, I. Chorkendorff, J.K. Norskov, Biomimetic hydrogen evolution: MoS_2 nanoparticles as catalyst for hydrogen evolution, J. Am. Chem. Soc., 127 (2005) 5308-5309.

[7] T.F. Jaramillo, K.P. Jorgensen, J. Bonde, J.H. Nielsen, S. Horch, I. Chorkendorff, Identification of active edge sites for electrochemical H2 evolution from MoS_2 nanocatalysts, Science, 317 (2007) 100-102.

[8] J. Peto, T. Ollar, P. Vancso, Z.I. Popov, G.Z. Magda, G. Dobrik, C. Hwang, P.B. Sorokin, L. Tapaszto, Spontaneous doping of the basal plane of MoS_2 single layers through oxygen substitution under ambient conditions, Nat Chem, 10 (2018) 1246-1251.

[9] Z. Wang, Q. Li, H. Xu, C. Dahl-Petersen, Q. Yang, D. Cheng, D. Cao, F. Besenbacher, J.V. Lauritsen, S. Helveg, M. Dong, Controllable etching of MoS_2 basal planes for enhanced hydrogen evolution through the formation of active edge sites, Nano Energy, 49 (2018) 634-643.

[10] S.S. Grønborg, K. Thorarinsdottir, L. Kyhl, J. Rodriguez-Fernández, C.E. Sanders, M. Bianchi, P. Hofmann, J.A. Miwa, S. Ulstrup, J.V. Lauritsen, Basal plane oxygen exchange of epitaxial MoS_2 without edge oxidation, 2D Materials, 6 (2019).

[11] J. Xie, J. Zhang, S. Li, F. Grote, X. Zhang, H. Zhang, R. Wang, Y. Lei, B. Pan, Y. Xie, Controllable disorder engineering in oxygen-incorporated MoS_2 ultrathin nanosheets for efficient hydrogen evolution, J. Am. Chem. Soc., 135 (2013) 17881-17888.

[12] P. Hou, D. Meeker, H. Wise, Kinetic studies with a sulfur-tolerant water gas shift catalyst, J. Catal., 80 (1983) 280-285.

[13] C.R.F. Lund, Microkinetics of Water−Gas Shift over Sulfided Mo/Al_2O_3 Catalysts, Industrial & Engineering Chemistry Research, 35 (1996) 2531-2538.

[14] H. Schweiger, P. Raybaud, G. Kresse, H. Toulhoat, Shape and Edge Sites Modifications of MoS_2 Catalytic Nanoparticles Induced by Working Conditions: A Theoretical Study, J. Catal., 207 (2002) 76-87.

[15] J. Lauritsen, J. Kibsgaard, G. Olesen, P. Moses, B. Hinnemann, S. Helveg, J. Norskov, B. Clausen, H. Topsoe, E. Lagsgaard, Location and coordination of promoter atoms in Co- and Ni-promoted MoS2-based hydrotreating catalysts, J. Catal., 249 (2007) 220-233.

[16] J.V. Lauritsen, M.V. Bollinger, E. Lægsgaard, K.W. Jacobsen, J.K. Nørskov, B.S. Clausen, H. Topsøe, F. Besenbacher, Atomic-scale insight into structure and morphology changes of MoS_2 nanoclusters in hydrotreating catalysts, J. Catal., 221 (2004) 510-522.

[17] A.S. Walton, J.V. Lauritsen, H. Topsøe, F. Besenbacher, MoS_2 nanoparticle morphologies in hydrodesulfurization catalysis studied by scanning tunneling microscopy, J. Catal., 308 (2013) 306-318.

[18] J. Bonde, P.G. Moses, T.F. Jaramillo, J.K. Norskov, I. Chorkendorff, Hydrogen evolution on nano-particulate transition metal sulfides, Faraday Discuss., 140 (2008) 219-231; discussion 297-317.

[19] Y.-Y. Chen, M. Dong, J. Wang, H. Jiao, On the Role of a Cobalt Promoter in a Water-Gas-Shift Reaction on Co-MoS_2, The Journal of Physical Chemistry C, 114 (2010) 16669-16676.

[20] Y.-Y. Chen, M. Dong, J. Wang, H. Jiao, Mechanisms and Energies of Water Gas Shift Reaction on Fe-, Co-, and Ni-Promoted MoS_2 Catalysts, The Journal of Physical Chemistry C, 116 (2012) 25368-25375.

[21] C. Zhang, B. Liu, L. Zhao, Q. Zong, J. Gao, Y. Wang, C. Xu, Insights into water–gas shift reaction mechanisms over MoS2 and Co-MoS_2 catalysts: a density functional study, Reaction Kinetics, Mechanisms and Catalysis, 120 (2017) 833-844.

[22] S. Yun, V.V. Guliants, Support Effects on Water Gas Shift Activity and Sulfur Dependence of Mo Sulfide Catalysts, Energy & Fuels, 33 (2019) 11655-11662.

[23] C. Hulteberg, Sulphur-tolerant catalysts in small-scale hydrogen production, a review, Int. J. Hydrogen Energy, 37 (2012) 3978-3992.

[24] J.A. Singh, S.H. Overbury, N.J. Dudney, M. Li, G.M. Veith, Gold Nanoparticles Supported on Carbon Nitride: Influence of Surface Hydroxyls on Low Temperature Carbon Monoxide Oxidation, ACS Catalysis, 2 (2012) 1138-1146.

[25] D. Lorito, A. Paredes-Nunez, C. Mirodatos, Y. Schuurman, F.C. Meunier, Determination of formate decomposition rates and relation to product formation during CO hydrogenation over supported cobalt, Catal. Today, 259 (2016) 192-196.

[26] E. Dominguez Garcia, J. Chen, E. Oliviero, L. Oliviero, F. Maugé, New insight into the support effect on HDS catalysts: evidence for the role of Mo-support interaction on the MoS_2 slab morphology, Applied Catalysis B: Environmental, 260 (2020).

[27] J. Chen, E. Dominguez Garcia, L. Oliviero, F. Maugé, How the CO molar extinction coefficient influences the quantification of active sites from CO adsorption followed by IR spectroscopy? A case study on MoS_2/Al_2O_3 catalysts prepared with citric acid, J. Catal., 332 (2015) 77-82.

[28] A. Travert, C. Dujardin, F. Maugé, S. Cristol, J.F. Paul, E. Payen, D. Bougeard, Parallel between infrared characterisation and ab initio calculations of CO adsorption on sulphided Mo catalysts, Catal. Today, 70 (2001) 255-269.

[29] D. Mey, S. Brunet, C. Canaff, F. Maugé, C. Bouchy, F. Diehl, HDS of a model FCC gasoline over a sulfided $CoMo/Al_2O_3$ catalyst: Effect of the addition of potassium, J. Catal., 227 (2004) 436-447.

[30] W. Chen, F. Maugé, J. van Gestel, H. Nie, D. Li, X. Long, Effect of modification of the alumina acidity on the properties of supported Mo and CoMo sulfide catalysts, J. Catal., 304 (2013) 47-62.

[31] L. Zavala-Sanchez, X. Portier, F. Mauge, L. Oliviero, High-resolution STEM-HAADF microscopy on a gamma-Al_2O_3 supported MoS_2 catalyst-proof of the changes in dispersion and morphology of the slabs with the addition of citric acid, Nanotechnology, 31 (2020) 035706.

[32] M. Badawi, J.F. Paul, S. Cristol, E. Payen, Y. Romero, F. Richard, S. Brunet, D. Lambert, X. Portier, A. Popov, E. Kondratieva, J.M. Goupil, J. El Fallah, J.P. Gilson, L. Mariey, A. Travert, F. Maugé, Effect of water on the stability of Mo and CoMo hydrodeoxygenation catalysts: A combined experimental and DFT study, J. Catal., 282 (2011) 155-164.

[33] N.C. Nelson, M.-T. Nguyen, V.-A. Glezakou, R. Rousseau, J. Szanyi, Carboxyl intermediate formation via an in situ-generated metastable active site during water-gas shift catalysis, Nature Catalysis, 2 (2019) 916-924.

[34] R.A. Ojifinni, N.S. Froemming, J. Gong, M. Pan, T.S. Kim, J.M. White, G. Henkelman, C.B. Mullins, Water-enhanced low-temperature CO oxidation and isotope effects on atomic oxygen-covered Au(111), J. Am. Chem. Soc., 130 (2008) 6801-6812.

[35] C. Rhodes, S.A. Riddel, J. West, B.P. Williams, G.J. Hutchings, The low-temperature hydrolysis of carbonyl sulfide and carbon disulfide: a review, Catal. Today, 59 (2000) 443-464.

[36] Z. George, Kinetics of cobalt-molybdate-catalyzed reactions of SO_2 with H_2S and COS and the hydrolysis of COS*1, J. Catal., 32 (1974) 261-271.

[37] L. Sharma, R. Upadhyay, S. Rangarajan, J. Baltrusaitis, Inhibitor, Co-Catalyst, or Co-Reactant? Probing the Different Roles of H_2S during CO_2 Hydrogenation on the MoS_2 Catalyst, ACS Catalysis, 9 (2019) 10044-10059.

Supporting Information. IR study of MoS_2/Al_2O_3 catalysts prepared with and without citric acid (CA) - Effect of H_2 treatment on sulfided $Mo(CA=2)/Al_2O_3$ - In-situ IR spectra during $H_2{}^{18}O$ treatment on sulfided $Mo(CA=2)/Al_2O_3$ - Effect of resulfidation - Formation of formate species on Mo/Al_2O_3 upon CO treatment - Decomposition of formate species on Mo/ Al_2O_3 - Post-treatment followed by CO/IR characterization - Spectra treatment and concentration of sites calculation.